(29) Bondi, A. *Physical Properties of Molecular Crystals, Liquids, and Gases*: Wiley: New York, 1968.
(30) Grolier, J.-P. E.; Ballet, D.; Viallard, A. *J. Chem. Thermodyn.* **1974**, *6*, 895.
(31) Otin, S.; Thomas, G.; Peiro, J. M.; Velasco, I.; Gutierrez Losa, C. *J. Chem. Thermodyn.* **1980**, *12*, 955.
(32) Dusart, O.; Piekarski, S.; Grolier, J.-P. E. *J. Chim. Phys. Phys.-Chim. Biol.* **1979**, *76*, 433.
(33) Polo, C.; Otin, S.; Gutierrez Losa, C.; Garcia, M. *J. Chim. Phys. Phys.-Chim. Biol.* **1977**, *74*, 152.
(34) Lai, T. T.; Doan-Nguyen, T. H.; Vera, J. H.; Ratcliff, G. A. *Can. J. Chem. Eng.* **1978**, *56*, 358.
(35) Zivny, A.; Biros, J.; Obereigner, B.; Pouchly, J. *J. Chim. Phys. Phys.-Chim. Biol.* **1975**, *72*, 379.
(36) Kauer, E.; Kirchner, D.; Haupt, D.; Bittrich, H. J. *Z. Phys. Chem. (Leipzig)* **1972**, *250*, 153.
(37) Polo, C.; Gutierrez Losa, C.; Kechavarz, M. R.; Kehiaian, H. V. *Ber. Bunsenges. Phys. Chem.* **1980**, *84*, 525.
(38) Doan-Nguyen, T. H.; Vera, J. H.; Ratcliff, G. A. *J. Chem. Eng. Data* **1978**, *23*, 218.
(39) Paz-Andrade, M. I.; Bravo, R.; Garza, M.; Grolier, J.-P. E.; Kehiaian, H. V. *J. Chim. Phys. Phys.-Chim. Biol.* **1979**, *76*, 51.
(40) Alessandrini, A.; Alessi, P.; Kikic, I. *Ann. Chim. (Rome)* **1980**, *70*, 293.
(41) Valero, J.; Garcia, M.; Gutierrez Losa, C. *J. Chem. Thermodyn.* **1983**, *15*, 985.
(42) Elliot, K.; Wormald, C. J. *J. Chem. Thermodyn.* **1976**, *8*, 881.
(43) Diaz Pena, M.; Menduina, C. *J. Chem. Thermodyn.* **1974**, *6*, 387.
(44) Muncsch, E. *Thermochim. Acta* **1978**, *22*, 237.
(45) Romani, L.; Paz-Andrade, M. I. *An. Quim.* **1974**, *70*, 422.
(46) Brown, I.; Fock, W.; Smith, F. *Aust. J. Chem.* **1964**, *17*, 1106.
(47) Nguyen, T. H.; Ratcliff, G. A. *J. Chem. Eng. Data* **1975**, *20*, 252.
(48) Bravo, R.; Paz-Andrade, M. I.; Kehiaian, H. V. *Acta Cient. Compostelana* **1979**, *16*, 141.
(49) Grolier, J.-P. E.; Sosnkowska-Kehiaian, K.; Kehiaian, H. V. *J. Chim. Phys. Phys.-Chim. Biol.* **1973**, *70*, 367.
(50) Larsen, B. L.; Fredenslund, A.; Rasmussen, P. *Wiss. Beitr.-Martin Luther Univ.*: Halle-Wittenberg: 1984; p 156.
(51) Weidlich, U.; Gmehling, J. *Ind. Eng. Chem. Res.* **1987**, *26*, 1372.
(52) Thomas, E. R.; Ekerdt, C. A. *Ind. Eng. Chem. Proc. Res. Dev.* **1984**, *23*, 194.
(53) Pimental, G. C.; McClellan, A. L. *The Hydrogen Bond*; W. H. Freeman: San Francisco, CA, 1960.
(54) Olabisi, O. *Macromolecules* **1975**, *8*, 316.
(55) Iskandar, M.; Tran, C.; Robeson, L. M.; McGrath, J. E. *Polymer Alloys, Blends, and Composites*; Society of Plastics Engineers, NATEC: Bal Harbour, FL, Oct 25-27, 1982; p 165.
(56) Nagata, J.; Nagashima, M.; Kazuma, K.; Nakagawa, M. *J. Chem. Eng. Jpn.* **1975**, *8*, 261.
(57) Woo, E. Ph.D. Dissertation, University of Texas at Austin, 1984.
(58) Sanchez, I. C. *Ann. Rev. Mater. Sci.* **1983**, *13*, 387.
(59) McMaster, L. P. *Macromolecules* **1973**, *6*, 760.
(60) Walsh, D. J.; Rostami, S.; Singh, B. *Makromol. Chem.* **1985**, *186*, 145.
(61) Walsh, D. J.; Rostami, S. *Macromolecules* **1985**, *18*, 216.
(62) Ten Brinke, G.; Karasz, F. E. *Macromolecules* **1984**, *17*, 815.
(63) Himmelblau, D. M. *Applied Non-linear Programming*; McGraw-Hill: New York, 1972.
(64) Luenberger, D. G. *Introduction to Linear and Non-linear Programming*, 2nd ed.; Addison-Wesley: Reading, MA, 1984.

Static and Dynamic Light Scattering Studies of Poly(terephthalic acid-4-aminobenzohydrazide) in Dimethyl Sulfoxide

W. R. Krigbaum and G. Brelsford*

Department of Chemistry, Duke University, Durham, North Carolina 27706.
Received December 10, 1987

ABSTRACT: Eleven narrow fractions between 3.78×10^3 and 2.62×10^5 g/mol of poly(terephthalic acid-4-aminobenzohydrazide) were studied in dimethyl sulfoxide. The molecular weight dependence of the intrinsic viscosity, molecular anisotropy, radius of gyration, and the diffusion coefficient, D_0, was used to derive a persistence length, q, of 105 ± 10 Å. The trend found in D_0, being less sensitive to chain expansion in a good solvent, supports the neglect of correcting molecular dimensions for the excluded-volume effect. An application of the Yamakawa-Stockmayer treatment for the expansion factor, α_s, for wormlike chains shows that the Kuhn limit is reached at nearly 6×10^4 g/mol while α_s^2 does not exceed 1.05 at a molecular weight of 2×10^5 g/mol.

Introduction

Workers at Monsanto developed a high modulus, heat-resistant fiber, X-500, by wet-spinning the poly(terephthalic acid-4-aminobenzohydrazide) from dimethyl acetamide (DMAC) or dimethyl sulfoxide (DMSO) with and without LiCl.[1] Even though the X-500 fibers attained high strength, their performance did not attain, much less exceed, that of Du Pont's Kevlar and X-500 was hence never commercialized.

An important distinction between these two materials exists with regard to their phase behavior in concentrated solution. Poly(*p*-phenylenediamine-terephthalic acid) (PPTA) forms a nematic liquid crystal at approximately 8% by weight in 96% sulfuric acid at 25 °C.[2] Optimum fiber properties result when spinning from 20% (wt/wt) solutions at 80 °C.[2] The ordered nematic phase assists in producing fibers having polymer chains highly oriented along the fiber direction. In contrast, a mesophase for the X-500/DMSO or DMAC systems (with or without added salt) is not observed even up to 27% (w/w) at 25 °C.[3] The solubility of X-500 decreases with increasing temperature.[3]

Table I
Literature Values Reported for the Persistence Length of X-500 in DMSO or DMAC at 25 °C

method	q, Å	ref
birefringence techniques	240-400	6-8
SLS	35-60 (70-80)	9
$[\eta]$	49 (70)	3
SAXS[a]	71-88 (90-98)[b]	10
SLS, $[\eta]$	100-120	11
flow birefringence	125	12
SLS, $[\eta]$	112	13

[a] Small-angle X-ray scattering. [b] DMAC.

X-500 is soluble in sulfuric acid but degrades in that solvent at room temperature. However, Morgan[4] observed a liquid crystal solution at a concentration of 10% (w/w) for X-500 in sulfuric acid at 0 °C. We are not aware of X-500 fiber produced under these conditions.

The difference in phase behavior between X-500 in DMSO at 25 °C and in H_2SO_4 at 0 °C suggests a more flexible chain in DMSO. The characterization of chain flexibility of X-500 in DMSO or DMAC at 25 °C has been

0024-9297/88/2221-2502$01.50/0

the subject of several investigations utilizing various techniques.[3,5-13] Values of the persistence lengths from these studies are summarized in Table I.

The lower values of q in Table I were obtained by estimating and applying a correction for the effects of chain expansion believed to be present in DMSO at 25 °C. Use of the correction seemed justified in light of large second virial coefficients, A_2, having a negative temperature dependence. It is well-known that when $A_2 = 0$, the expansion factor, α, equals unity. Under such conditions, the polymer chains attain unperturbed dimensions.[14] The most recent studies[11-13] reported for X-500 have neglected a correction for the excluded-volume effect. The newer results stand in good agreement with one another and in fair agreement with earlier results for q without correcting for expansion. (See values in parentheses in Table I).

The present study characterizes the persistence length of X-500 in DMSO using dynamic light scattering (DLS). DLS permits a determination of translational diffusion coefficients, $\bar{D}$. In the limit of infinite dilution, $\bar{D}$ is inversely proportional to the friction coefficient (f_0) of the molecule. The friction coefficient scales as the radius of the molecule to the first power, whereas the radius of gyration, $\langle s^2 \rangle_z$, and intrinsic viscosity, $[\eta]$, scale with the radius, and hence α, to some higher power.[14] From these considerations, the value of q derived from the measurement of D_0 should be less sensitive to the excluded-volume effect.

In addition, static light scattering (SLS) and $[\eta]$ measurements performed on the same fractions allow a comparison of trends in $[\eta]$, $\langle s^2 \rangle_z$, and molecular anisotropy (δ) versus molecular weight with data in the literature. A comparison of values for q derived from these trends with the q found from the DLS data should provide evidence regarding the nature of chain dimensions of X-500 in DMSO.

Experimental Section

X-500 was supplied by Monsanto. The polymer was fractionated by successive precipitation. Initially, several grams of polymer were dissolved in Fisher reagent grade DMSO to a concentration of 1 g/dL. Ethyl acetate was slowly added to the solution until the cloud point was observed. As was found by Sakurai et al., the liquid mixture had to be cooled in order to redissolve the fraction.[13] The liquid was then allowed to equilibrate to room temperature until a gel settled to the bottom of the fractionation vessel. The gel was separated from the liquid and precipitated with methanol. Fractions obtained successively in this manner were dried in a vacuum oven at room temperature for 1 week.

Intrinsic viscosity and light scattering measurements were performed on solutions prepared with doubly distilled DMSO. The viscosity of DMSO at 23 °C was measured with a calibrated Cannon-Ubbelohde viscometer. Stock solutions were prepared for each fraction and stored in a drybox over P_2O_5 until use. For the most part SLS and DLS measurements were performed on the same samples.

A syringe fitted with a Millipore Swinney 13-mm stainless steel filter unit holding either type FG or FH Teflon filters was used to filter dust from samples investigated by light scattering. Solutions filtered into light scattering cells were centrifuged in a Sorvall bench-top centrifuge to pull any remaining dust to the bottom of the cell and oub of the path of the laser beam.

The refractive index increment, dn/dc, was measured at three wavelengths: 435.6, 546, and 632.8 nm, using a Brice-Phoenix differential refractometer. Data were collected on several fractions by using various concentrations within the range used for light scattering measurements (5×10^{-4} to 6×10^{-3} g/mL).

The light source for our light scattering instrument is a Coherent INNOVA 90-3 argon ion laser. We used the 514.5-nm line to avoid absorption of the incident light known to occur for X-500 in solution at lower wavelengths.[5] Vertically polarized incident light is focused by a 15-cm focal length lens into the center of a Brookhaven Instruments Model E083 temperature controlled vat. Borosilicate glass tubes, 12 mm, fitted with ground-glass joints serve as sample cells.

The vat is mounted on an x–y translation stage to allow positioning of the sample on the geometric center of a modified Picker X-ray goniometer. The goniometer is fastened and leveled to the top of a Newport Research Corporation optical table. The goniometer supports and rotates an optical rail on which the detection optics are situated. The detection optics are housed in a Malvern RR109 detector assembly. The RR109 was modified to accommodate an analyzer in order to define the polarization of the scattered light. The optimum high voltage to an ITT FW 130 photomultiplier tube (PMT) is supplied by an Ortec Model 446 power supply. The signal from the PMT is registered on a 128 channel Malvern K7025 multibit correlator. The time-averaged photocounts are obtained from the correlator imput channel for SLS. Alternatively, the autocorrelation function of time-dependent fluctuations in the scattered intensity is retrieved from the 128 data channels for DLS measurements. The correlator is interfaced to a Vector Graphics Scientific computer via a Pickles & Trout IEE 488 interface card. Separate programs automate data collection for both SLS and DLS. The analog output of the correlator permits a display of the accumulating correlation function on an oscilloscope. Details of instrumental tests on standard anionic polystyrene dissolved in toluene and polystyrene latex spheres suspended in water are given elsewhere.[15]

Results

Static Light Scattering. Excess intensities $I_{ex}(\theta)$ measured between $\theta = 30°$ and 140° were converted to Rayleigh ratios $R_{v,v}(\theta)$ by using

$$R_{v,v}(\theta) = (n_s/n_v)^2(R_{cal}/I_{cal})(I_{ex}) \sin(\theta) \quad (1)$$

where n_s and n_v are the refractive indices of the solvent (DMSO = 1.476) and index matching fluid in the vat (xylene = 1.497), respectively. R_{cal} and I_{cal} are the Rayleigh ratio and intensity of the calibrating liquid, respectively. The sin (θ) factor corrects for the change in size of the scattering volume with scattering angle θ. The subscript v,v denotes vertically polarized incident and scattered light. The value taken for R_{cal} of toluene at 514.5 nm was 24.0×10^{-6} cm^{-1}.[15]

Zimm plots were used to determine apparent molecular weights, M_{app}, second virial coefficients, $A_{2,app}$, and radii of gyration, $\langle s^2 \rangle_{app}$, according to

$$\lim_{\theta,c\to 0} \frac{Kc}{R_{v,v}(\theta)} = M_{app}^{-1}[1 + 2A_{2app}M_{app}c + (1/3)k^2\langle s^2 \rangle_{app}] \quad (2)$$

$$k = \frac{4\pi}{\lambda} \sin \frac{\theta}{2} \quad (3)$$

$$K = \frac{4\pi^2 n_s^2}{N_A \lambda_0^4}\left(\frac{dn}{dc}\right)^2 \quad (4)$$

where k is the magnitude of the scattering vector and $\lambda = \lambda_0/n_s$ is the wavelength of light in the medium. The optical constant, K, contains the wavelength of incident light λ_0 in vacuo, n_s, and the square of dn/dc. c is the concentration expressed in grams per milliliter and N_A is Avagodro's number.

The literature values of dn/dc for X-500 in DMSO at 546 and 435.8 nm are collected in Table II. Bianchi et al.[3] noted that the refractive index increment was sensitive to water content. This perhaps explains the wide range of values for dn/dc observed. Figure 1 shows the present results at three wavelengths plotted versus λ^{-2}. From a linear least-squares fit to the data, dn/dc at 514.5 nm is 0.210 mL/g.

The angular dependent data, in the limit of infinite dilution, are collected from the Zimm plots and illustrated

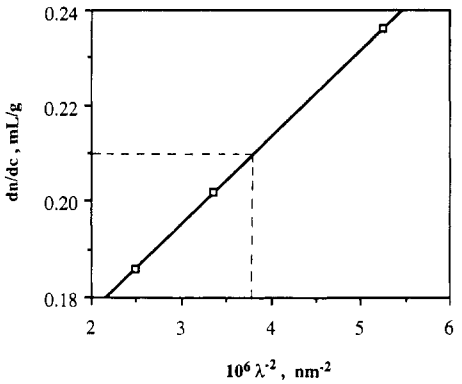

Figure 1. Refractive index increment of X-500 in DMSO at room temperature versus λ^{-2}. dn/dc at 514.5 nm = 0.210.

Table II
Literature Values for the Refractive Index Increment of X-500 in DMSO Measured at 25 °C

λ, nm	dn/dc, mL/g	ref
546	0.166	5
	0.175	9
	0.180	11
	0.205	13
435.8	0.240	13

in Figure 2 for fractions 1–6 and 8. The $\langle s^2\rangle_{app}$ for fraction 7 was not reported due to large uncertainty in the angular dependent data caused by dust. Fractions 9–11 did not show any angular dependence and were measured at θ = 90°. Apparent molecular weights, radii of gyration, and second virial coefficients are given in columns 2–4 to Table III.

M_{app}, $\langle s^2\rangle_{app}$, and $A_{2,app}$ were corrected for the effects of depolarization by using the Berry method.[16] The depolarization ratio ρ_v, in the limit of infinite dilution and zero scattering angle, is related to the total molecular anisotropy, δ^2, by

$$\delta^2 = \frac{5\rho_v}{(3 - 4\rho_v)} \tag{5}$$

The values calculated for δ^2 are given in column 5 of Table III. Equations 6–8 were used to correct apparent

$$\langle M\rangle_w = M_{app}/(1 + (4/5)\delta^2) \tag{6}$$

$$\langle s^2\rangle_z = \frac{\left(1 + \frac{7}{5}\delta^2\right)\langle s^2\rangle_{app}}{\left(1 - \frac{4}{5}f_1\delta + \frac{4}{7}f_2\delta^2\right)} \tag{7}$$

$$A_2 = A_{2,app}\left(1 + \frac{4}{5}\delta^2\right)^2 \tag{8}$$

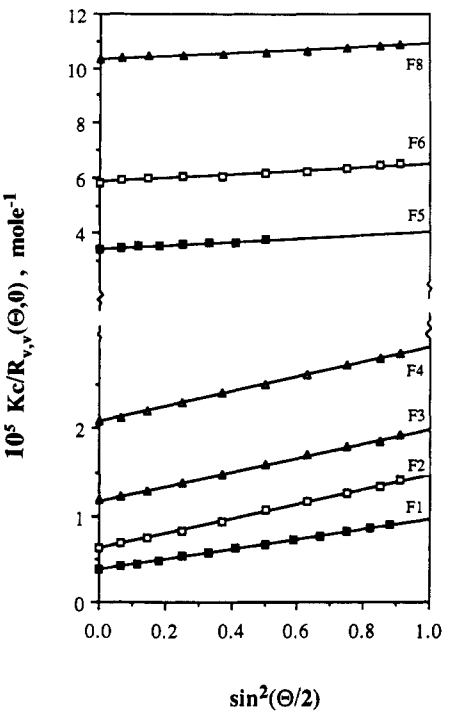

Figure 2. Angular dependence of $Kc/R_{v,v}(\theta,c)$ at c = 0 for fractions 1–6 and 8.

values for the effects of depolarization, where f_1 and f_2 are functions of the number of persistence lengths in the chain. Corrected apparent molecular weights and second virial coefficients are given in columns 6 and 7 of Table III, respectively. The parameters f_1 and f_2 equal unity for ideal anisotropic rigid rods and approach zero for random coils.[16] Values for $\langle s^2\rangle_z$ calculated by using f_1 and f_2 equal to 1 are given in column 8 of Table III. The values in parentheses were calculated by using f_1 and f_2 equal to 0 and are within the estimated experimental error (<5%) of the $\langle s^2\rangle_{app}$ values.

Dynamic Light Scattering. Measured time correlation functions were analyzed by the method of cumulants.[17] The average decay rate ($\bar{\Gamma}$) is related to the z-average translational diffusion coefficient by

$$\bar{\Gamma} = \bar{D}k^2 \tag{9}$$

The sample time Δt for DLS measurements of X-500 solutions at 23 °C was set by using the criterion $\Delta t = 3/128\bar{\Gamma}$.[18] Correlation functions were collected until contents of the second data channel were on the order of 10^5 above base lines of 10^6. Agreement between the theoretical and measured base lines within 0.2%, low reduced χ^2 values, and relative standard deviations in $\mu_2/\bar{\Gamma}^2$ below 15–20% were used to assess the quality of the second order cumulants fit in determing $\bar{\Gamma}$.

Table III
Results from Static Light Scattering Measurements on X-500 Fractions in DMSO at 23 °C

fraction	$10^{-3}M_{w,app}$, g mol^{-1}	$10^3A_{2,app}$, cm^3 mol g^{-2}	$10^{-3}\langle s^2\rangle_{z,app}$, Å^2	$10^2\delta^2$	$10^{-3}\langle M\rangle_w$, g mol^{-1}	10^3A_2, cm^3 mol g^{-2}	$10^{-3}\langle s^2\rangle_z$, Å^2
1	262	3.26	357	0.590	260	3.27	380 (358)
2	157	1.70	311	1.09	155	1.71	339 (313)
3	84.8	4.93	160	1.30	83.9	4.98	176 (161)
4	47.9	5.50	87.3	1.95	47.1	5.59	98.5 (88.6)
5	29.2	5.81	46.4	2.83	28.5	5.94	53.8 (47.4)
6	17.2	4.27	26.5	4.40	16.6	4.42	31.9 (27.4)
7	10.2	3.90		5.21	9.79	4.06	
8	9.66	5.43	11.8	6.76	9.16	5.72	14.9 (12.4)
9	7.48	6.01		7.36	7.06	6.36	
10	6.12	4.90		9.83	5.67	5.29	
11	4.19	7.11		13.3	3.78	7.87	

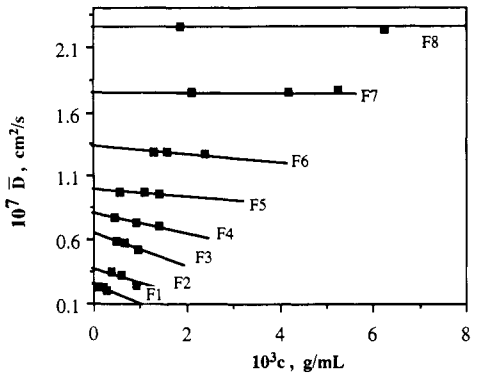

Figure 3. Concentration dependence of diffusion coefficients for fractions 1–8.

Table IV
Results from Dynamic Light Scattering Measurements on X-500 Fractions in DMSO at 23 °C

fraction	$10^8 D_0$, cm² s⁻¹	R_H, Å	k_D, cm³ g⁻¹	$\mu_2/\bar{\Gamma}^2_{c,\theta\to 0}$
1	2.55	405	−588	0.121
2	3.93	263	−349	0.112
3	6.55	158	−192	0.026
4	8.06	128	−101	0.022
5	10.0	103	−31.0	0.148
6	13.2	78.3	−16.2	0.025
7	17.5	59.1		0.096
8	22.5	45.9		0.089
9	22.8	45.3		
10	29.7	34.8		
11	40.2	25.7		

The angular dependence for $\bar{D}$ was linear below $\theta = 60°$. This result is in agreement with the relationship characterizing the regime where the signal due to translational diffusion is adequately separated in frequency from rotational and flexing modes which occur on shorter time scales, i.e., $k\langle s^2\rangle_z^{1/2} < 1$.[19] $\bar{D}$ is plotted versus c in Figure 3 for fractions 1–8. The concentration dependence of $\bar{D}$ is expressed as $\bar{D} = D_0(1 + k_D c)$. Values of k_D in column 4 of Table IV are negative and approach zero as $\langle M\rangle_w$ decreases.

Diffusion coefficients in the limit of infinite dilution, D_0, are given in column 2 of Table IV. A single concentration, well below the overlap concentration c^* ($\sim[\eta]^{-1}$) was measured and taken as D_0 for fractions 9–11. Hydrodynamic radii, R_H, calculated from the Stokes–Einstein equation, using 0.0210 P for the viscosity of DMSO at 23 °C, are listed in column 3 of Table IV.

The normalized second cumulant ($\mu_2/\bar{\Gamma}^2$) is related to the distribution of decay rates. We have made use of the relation in eq 10 between $\mu_2/\bar{\Gamma}^2$ (in the limit of infinite dilution and zero scattering angle) and the ratio of weight to number-average molecular weights for rodlike particles, derived by Kubota and Chu, to estimate sample polydispersity.[20] The use of eq 10 here is intended only to provide

$$\langle M\rangle_w/\langle M\rangle_n = 1 + \lim_{\theta,c\to 0} \mu_2/\bar{\Gamma}^2 \qquad (10)$$

an estimate of sample polydispersity in contrast to methods used to determine molecular weight distributions quantitatively.[21] Limiting values of $\mu_2/\bar{\Gamma}^2$ are reported in column 5 of Table IV.

Instrinsic Viscosity. Table V summarizes values of $[\eta]$, k', and $-k''$ for X-500 fractions in DMSO at 25 °C. The $[\eta]$ for fraction 2 was estimated from the flow time of a single concentration and the average k' value, 0.15. A log–log plot of $[\eta]$ versus $\langle M\rangle_w$ revealed that the Mark–Houwink exponent decreases from 1.13 when $\langle M\rangle_w < 2 \times 10^4$ g/mol to 0.75 when $\langle M\rangle_w > 4 \times 10^4$ g/mol. Values

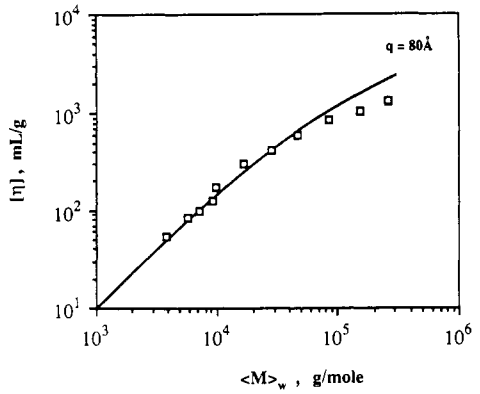

Figure 4. Molecular weight dependence of intrinsic viscosities for X-500 in DMSO at 25 °C. The solid curve was calculated with the Yamakawa–Fujii treatment[25] using d = 5.1 Å, M_L = 18.2 Å⁻¹, and q = 80 Å.

Table V
Results from Intrinsic Viscosity Measurements at 25 °C on X-500 Fractions in DMSO

fraction	$[\eta]$, dL g⁻¹	k'	$-k''$
1	13.4	0.323	0.175
2	10.5		
3	8.5	0.360	0.141
4	6.08	0.354	0.146
5	4.23	0.330	0.168
6	3.02	0.386	0.123
7	1.75	0.327	0.122
8	1.25	0.320	0.178
9	0.992	0.393	0.117
10	0.837	0.334	0.178
11	0.530	0.327	0.122

of the viscosity constant given by $\Phi = [\eta]\langle M\rangle_w/(6\langle s^2\rangle_z)^{3/2}$ were below 1.02×10^{23}/mol for all fractions. This value of Φ is well below theoretical values corresponding to unperturbed coils in the limit of infinite molecular weight.[14] This indicates that the solvent drains through the domain occupied by segments of a polymer molecule. We note that the present study extends the range of molecular weights reported for X-500 by a factor of 4.

Discussion

Determination of the Persistence Length. The Kratky–Porod wormlike chain model is employed most often in characterizing polymers having extended chains.[22] Two reviews by Yamakawa describe several treatments used to derive wormlike chain parameters.[23,24] Four of those methods are used here to determine the persistence length of X-500 in DMSO.

We begin with the Yamakawa–Fujii theory of intrinsic viscosity for wormlike cylinders unperturbed by the excluded-volume effect.[25] The theory applies to Oseen–Burgers procedure to wormlike chains of contour length L, hydrodynamic diameter d, and mass per unit length M_L. M_L was taken as 18.2 Da/Å (Da = dalton) corresponding to the ratio of the molecular weight of the repeat unit (M_0 = 281 g/mol) to the length of the repeat projected onto the contour of the chain (l_0 = 15.4 Å). M_L is related to the contour length by

$$\langle M\rangle_w/M_L = \langle L\rangle_w \qquad (11)$$

Assuming a circular cross-section for the chain, a chain diameter of 5.1 Å was calculated according to

$$d = (4M_L/\pi N_A \rho_2)^{1/2} \qquad (12)$$

where ρ_2 is the polymer density (1.48 g/mL).[3]

The best fit of the $[\eta]$ versus $\langle M\rangle_w$ data using these values for M_L and d was obtained with a q of 80 Å as seen

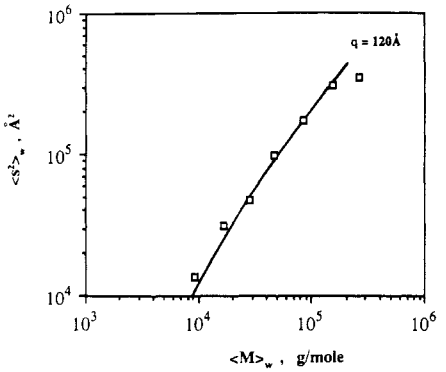

Figure 5. Molecular weight dependnece of the mean-square radius of gyration. The solid curve shows the result from the Benoit–Doty theory using q = 120 Å and M_L = 18.2 Da/Å.

Table VI
Estimated Corrections to $\langle s^2 \rangle_z$ Values for the Effects of Polydispersity in X-500 Fractions

fraction	$10^{-3}\langle s^2 \rangle_z$, Å^2	h	$10^{-3}\langle s^2 \rangle_w$, Å^2
1	380	8.26	343
2	339	8.93	308
3	176	38.5	172
4	98.5	45.5	96.4
5	53.8	6.76	47.7
6	31.9	40.0	31.1
8	14.9	11.2	13.8

in Figure 4. This value of q, as expected, is in fair agreement with other data uncorrected for the excluded-volume effect.[11-13]

The Benoit–Doty theory utilizes the wormlike chain model to express $\langle s^2 \rangle_z$ as a function of the contour and persistence lengths given by[26]

$$\langle s^2 \rangle_z = Lq/3 - q^2 + 2q^4(1 - \exp(-L/q))/L^2 \quad (13)$$

The quantities L and $\langle s^2 \rangle_z$ require a correction to common averages. The Schultz–Zimm distribution, given by $(\langle M \rangle_w/\langle M \rangle_w) - 1 = h^{-1}$, was used to convert values of $\langle s^2 \rangle_z$ for each fraction to their corresponding w-average by $\langle s^2 \rangle_w = \langle s^2 \rangle_z(h + 1)/(h + 2)$.[27] The $\langle s^2 \rangle_z$ values, calculated by using f_1 and f_2 equal to 1, were used and are collected with their corresponding h and $\langle s^2 \rangle_w$ values in Table VI.

Use was made of the relation for $\langle L \rangle_w$ along with eq 13 to derive a best fit of the $\langle s^2 \rangle_w$ data versus $\langle M \rangle_w$ in the log–log plot shown in Figure 5. The curve calculated by using q = 120 Å provides a best fit to the trend. This value of q is in excellent agreement with Tsvetkov et al.[11] and Sakurai et al.[13] This result is encouraging in that each study has corrected for depolarization and polydispersity by using different methods.

Values measured for fraction 2 were chosen to compute q in the Kuhn limit ($2q = A$, where A is the Kuhn segment length) as expressed by

$$q = 3\langle s^2 \rangle_w/L_w \qquad q = 108 \text{ Å} \quad (14)$$

This fraction is 2.5 times larger in $\langle M \rangle_w$ than the maximum reported for X-500 in the literature. This value of q is in agreement with the value determined from the trend in the lower $\langle M \rangle_w$ samples where it is sometimes assumed that $A = 2q$.

The measured trend of δ^2 versus the number of repeat units, N_w, in the chain provides another estimate of chain extension. Arpin et al.[28] evaluated δ^2 for a wormlike chain as a function of the segment or repeat unit anisotropy, δ_o^2, and the ratio of the contour length to the persistence length, i.e., $X = L/q$.[28] For a rodlike molecule, the model gives $\delta^2 = \delta_0^2$. For a molecule without any correlation in orientation between successive segments, the model predicts $\delta^2 = \delta_0^2/N_w$. The wormlike chain result can be expressed by

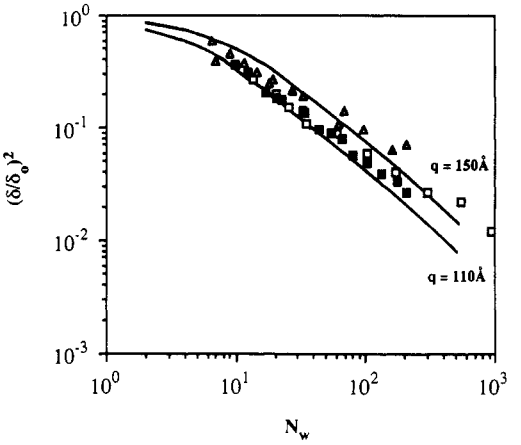

Figure 6. Plot of the total molecular anisotropy divided by the segment anisotropy, quantity squared, versus the number of repeat units according to the treatment of Arpin et al.[28] δ_0^2 = 0.49. Values of q are attached to the curves. (△) literature data for PPDT in H_2SO_4;[28,29] (■) data of Sakurai et al.[13] for X-500 in DMSO; (□) present results for X-500 in DMSO.

$$\delta^2 = \delta_0^2\{2/x' - 2/x'^2[1 - \exp(-x')]\} \quad (15)$$

where $x' = 3N_w l_0/q$. Note that $L = N_w l_0$.

The values of δ^2 for each fraction from Table III were divided by δ^2 = 0.49 and plotted versus N_w ($=\langle M \rangle_w/M_0$) in Figure 6. This value of δ_0^2 was determined by the iterative method of Sakurai et al.,[13] whose data are shown for comparison with the present results. It is interesting to note that Ying and Chu reported the same value of δ_0^2 for PPDT in H_2SO_4.[29] This fact suggests a direct comparison of molecular anisotropy data collected for the two polymers in their respective solvents.

The data of Arpin et al.[28] for fractionated and unfractionated PPTA and that of Ying and Chu[29] for unfractionated samples are also shown in Figure 6. Although the relationship between δ^2 and polydispersity is not known, we applied a correction to δ^2 for unfractionated PPTA samples assuming δ^2 to be a z-average quantity. The correction of δ^2 to a w-average was similar to that used earlier to correct $\langle s^2 \rangle_z$ to its estimated w-average for X-500 fractions, except that the value 1.8 was taken as the $\langle M \rangle_w/\langle M \rangle_n$ ratio for PPTA.[30]

The full curves represent the function $(\delta/\delta_0)^2$ plotted in a log–log fashion versus N_w. The parameters used to fit the X-500 data were l_0 = 15.4 Å, M_0 = 281 g/mol, and q = 110 Å. The best fit to the PPTA data was obtained with l_0 = 12.9 Å, M_0 = 238 g/mol, and 150 Å. The molecular anisotropy technique demonstrates that PPTA is about 1.5 times as stiff (in terms of the persistence length) as X-500 in their respective solvents near room temperature.

Again, the excluded-volume effect is neglected in deriving these values. However, in order to obtain a q = 50 Å for X-500, δ_0^2 would equal unity, corresponding to a totally anisotropic segment. It seems unlikely that this would be the case for the X-500 repeat unit. Berry used this method to study poly(p-phenylenebenzobisthiazole) (PBT) in methane sulfonic acid.[16] PBT is a ladder polymer having a very rigid backbone. With δ_0^2 = 1, q was found to be ≃1500 Å. Ying and Chu also reported tghe persistence length of poly(1,4-benzamide) (PBA) in DMAC/3% LiCl equal to ≃750 Å using δ_0^2 = 0.94.[31] Evidence of extended chain behavior is reflected not only in the magnitude of q, but also in the proximity of δ_0^2 to unity.

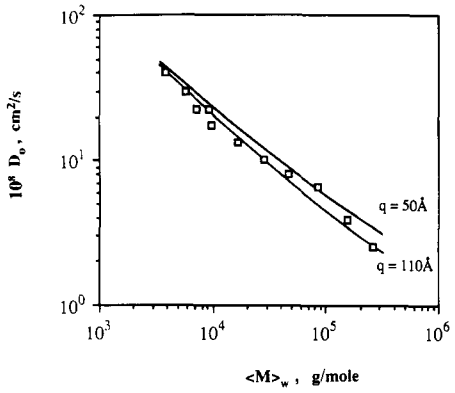

Figure 7. Molecular weight depenence of diffusion coefficients in the limit of infinite dilution compared to the theory of Yamakawa and Fujii.[32] Values of the persistence length are indicated on the plot. M_L = 18.2 Da/Å, d = 5.1 Å, and $\eta_{0,DMSO}$ = 0.0210 P at 23 °C.

Another treatment by Yamakawa and Fujii calculates the friction coefficient, f_0, for unperturbed wormlike chains in the limit of infinite dilution.[32] Their analytical equations, eq 49–52, permit a calculation of theoretical curves to fit the measured trend in f_0 versus $\langle L\rangle_w$. The function f_0 depends on q, d, and $\langle L\rangle_w$. A best fit to the D_0 data is used to derive an estimate of q for X-500 by using d = 5.1 Å, M_L = 18.2 Å^{-1}, and $\eta_{0,DMSO}$ = 0.0210 P at 23 °C. A log–log plot of the D_0 from Table IV versus $\langle M\rangle_w$ is shown in Figure 7. Each value of the persistence length is attached to its corresponding theoretical curve.

The full curves imply that f_0 is sensitive to $\langle L\rangle_w$ or $\langle M\rangle_w$. This was noted by Vitovskaya et al. in studies of PBA in H_2SO_4 and DMAC.[33] Inspection of their data shows that q could range from 150 to 1500 Å. Their conclusion stated that this treatment could be used to determine $\langle M\rangle_w$ for PBA more readily than q.

As seen in Figure 7, the curves are relatively insensitive to q. However, the D_0 data for X-500 below $\simeq 3 \times 10^4$ g/mol do tend to follow the curve for q = 110 Å. Above $\simeq 4 \times 10^4$ g/mole the data begin to scatter. This is unfortunate with regard to measuring D_0 closer to the coil limit. Nevertheless, we note that all but one of the samples studied by Bianchi et al.[3,9] were below 4×10^4 g/mol. The excluded-volume correction was applied to their data resulting in the low values of q cited in Table I.

A least-squares fit to all of the D_0 data gives $D_0 = 5.56 \times 10^{-4}\langle M\rangle^{-0.61}$ cm^2/s. For comparison, the data for PPTA scales as $D_0 = 2.11 \times 10^{-5}\langle M\rangle_w^{-0.75}$ cm^2/s in H_2SO_4 at 30 °C for $\langle M\rangle_w$ between 2.27×10^4 and 4.83×10^4 g/mol.[34] For PBA in DMAC/3% LiCl between 2.88×10^4 and 22.9×10^4 g/mol, the relationship was $D_0 = 1.24 \times 10^{-3}\langle M\rangle_w^{-0.89}$ cm^2/s.[31] For the present results, the exponent, a_D, in the $\langle M\rangle_w$ range below 3×10^4 g/mol is 0.72. Above 3×10^4 g/mol, the relation is $D_0 = 5.95 \times 10^{-4}\langle M\rangle_w^{-0.61}$ cm^2/s.

The exponent $a_D \simeq 0.7$ is large compared to coiling polymers in good solvents where $a_D \simeq 0.6$. For example, Selser measured poly(α-methylstyrene) in toluene at 25 °C from 5×10^3 to 1×10^6 g/mol.[35] a_D was equivalent to the unperturbed value, 0.5, for $\langle M\rangle_w$ values up to 10^5 g/mol. Since q for coiling polymers is $\simeq$15 Å, it seems unlikely that the DLS results for X-500 in DMSO are representative of the excluded-volume behavior exhibited by flexible coils in a good solvent.

Consideration of the Expansion Factor and the Second Virial Coefficient. The theory of Yamakawa and Stockmayer utilizes the wormlike chain model to derive expressions for the expansion factor α and A_2.[36] Both α and A_2 are functions of the excluded-volume parameter, z. We consider first the relationship between α and z in a qualitative yet informative manner.

In terms of the radius of gyration, α is defined by

$$(\langle s^2\rangle_z/\langle s_0^2\rangle_z)^{1/2} = \alpha_s \tag{16}$$

where the subscript 0 refers to unperturbed dimensions. α_s is related to z in the modified Flory treatment[14] for random coils by

$$\alpha_s^5 - \alpha_s^3 = \frac{134}{105}z \tag{17}$$

If α_s is close to unity, eq 17 can be written in the form

$$(\alpha_s^2 - 1) = \frac{134}{105}z \tag{18}$$

For wormlike chains, the result for α_s is given by the expression

$$(\alpha_{s,worm}^2 - 1) = \frac{67}{70}K(L/A)z \tag{19}$$

where $K(L/A)$ is a function of the number of Kuhn segment lengths in the chain. $K(L/A)$ approaches the value 4/3 as L/A approaches infinity, attaining equivalence with eq 18. Therefore, the ratio of α_s^2 for wormlike chains to α_s^2 for coils approaches unity as the function $K(L/A)$ approaches the value 4/3. Values for $K(L/A)$ are given in Table I of ref 36.

The ratio of $\langle s^2\rangle_w$, measured or calculated for wormlike chains, to the value of $\langle s^2\rangle_w$ in the coil limit, i.e., $\langle s^2\rangle_{w,coil} = Lq/3$, also approaches unity. This ratio, given by $3\langle s^2\rangle_w/Lq$, was calculated by using the experimental results for $\langle s^2\rangle_w$ given in Table VI with q = 120 Å. The slope of a plot of the hydrodynamic radius, R_H, versus $\langle s^2\rangle_w^{1/2}$ for fractions 2–6 and 8 was 0.45 ± 0.05. Estimates of $\langle s^2\rangle_w$ from this value and R_H values for the remaining fractions too small to exhibit any angular dependence by SLS were thus obtained.

Both ratios, $(3/4)K(L/A)$ and $3\langle s^2\rangle_w/Lq$, are plotted versus L/A on a log–log scale in Figure 8. The function $(3/4)K(L/A)$ is representd by the solid line to the right. Experimental results are shown by the square symbols. The solid line to the left represents the ratio $3\langle s^2\rangle_w/Lq$, calculated by using the Benoit–Doty expression. It is seen that the data for X-500 and a wormlike chain with q = 120 Å approaches the Kuhn limit at $L/A \simeq 15$, corresponding to $\langle M\rangle_w \simeq 6 \times 10^4$ g/mol.

The function $(3/4)K(L/A)$ approaches the Kuhn limit at a much higher L/A. Since we have not directly measured α_s^2, we resort to an estimation of this quantity. This requires an approximation of z, which we give below in eq 24. With β' = 298 nm^3 and A = 220 Å, α_s^2 at L/A = 15 is estimated to be 1.027. α_s^2 is predicted to become appreciable ($\alpha_s^2 > 1.05$) when $\langle M\rangle_w$ exceeds 2×10^5 g/mol.

If expansion were appreciable (i.e., measurable) in the present range of $\langle M\rangle_w$ studied, the $\langle s^2\rangle_w$ data would show a positive deviation from the Benoit–Doty equation.[37] Combining the absence of this observation with the insight from Figure 8, it is concluded that the low values of q in Table I, derived by applying a correction for α based on flexible coils, produced a value too low to represent the semiflexible nature of X-500 in DMSO.

An examination of the second virial coefficient provides further evidence regarding the nature of X-500 in DMSO. First, we consider the classic result derived by Zimm for hard rods[38]

$$A_2 = \pi N_A d L^2/4\langle M\rangle_w^2 \tag{20}$$

According to eq 20, A_2 is a constant versus $\langle M\rangle_w$ for rods

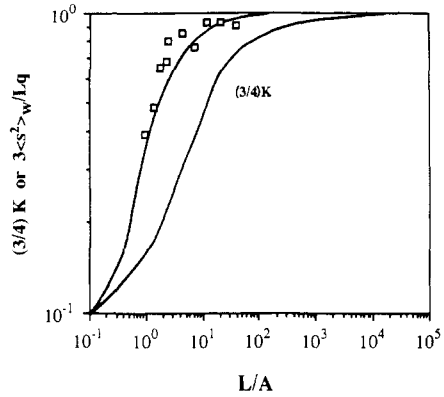

Figure 8. Function $(3/4)K$ or $3\langle s^2\rangle_w/Lq$ versus L/A. The function $(3/4)K$ is represented by the labeled curve to the right. $\langle s^2\rangle_w$ was calculated with eq 13 by using $q = 120$ Å for values of L in the measured range and is represented by the solid line on the left. Open squares represent experimental values of $\langle s^2\rangle_w$ used to calculate $3\langle s^2\rangle_w/Lq$.

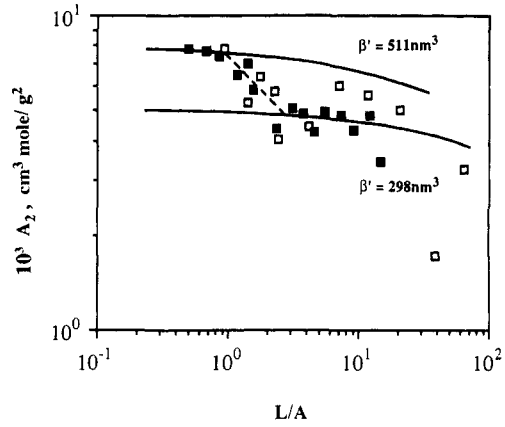

Figure 9. Second virial coefficient data for X-500 in DMSO versus the number of Kuhn segments in the chain. Values of β' are attached to the solid curves calculated by using $A = 220$ Å: (□) present results; (■) Sakurai et al.[13]

since $\langle M\rangle_w \sim \langle L\rangle_w$. By substituting $\langle L\rangle_w M_L = \langle M\rangle_w$ we find that $A_2 = \pi N_A d/4M_L^2$. Inserting the appropriate values for X-500 yields the constant 7.28×10^{-3} cm³ mol/g².

The present results for A_2, along with the data of Sakurai et al.,[13] are plotted versus the number of Kuhn segments, L/A, in Figure 9. Below $L/A = 1$ the data are in good agreement with the value predicted by using eq 20. Between $L/A = 1$ and 2, the A_2 data exhibit a marked decrease. Up to about $L/A = 15$, and above $L/A = 2$, the data scatter about an average value of 4.8×10^{-3} cm³ mol/g².

We therefore turn to the Yamakawa–Stockmayer treatment of A_2 for wormlike chains.[36] Their calculations are based on and array of beads superimposed along a wire obeying wormlike chain statistics. The relationship for A_2 is

$$A_2 = (N_A L^2 B'/2\langle M\rangle_w^2)h \qquad (21)$$

where B' is a parameter having units of length. The function h is represented by

$$h = 1 - Q(L_r)z + \ldots \qquad (22)$$

$$Q(L_r) = 2(L_r)^{-5/2}H(L_r,d_r) \qquad (23)$$

where $H(L_r,d_r)$ is given by eq 119 of ref 36. The subscript r denotes unitless dimensions such that $L_r = L/A$ and $d_r = d/A$.

The excluded-volume parameter z is defined by using eq 24, where β' is the binary cluster integral having di-

$$z = (3/2\pi A^2)^{3/2}\beta'(L_r)^{1/2} \qquad (24)$$

mensions of volume. The correspondence between β' and B' is given by $\beta' = B'A^2$ if the beads on the wire are separated by the distance A. Since the significance of this is not clear, we simply treat β' as a fitting parameter. We note that Huber and Stockmayer have used a similar approach in calculating z for polystyrene in toluene.[39] These workers found that a larger value of β' was required to fit the A_2 data below $\langle M\rangle_w = 10^4$ g/mol than the value required above 10^5 g/mol.[39]

We report a similar finding in the case of X-500 in DMSO in Figure 9. The solid curves represent calculations performed by using $A = 22$ nm and two separate values of β', 511 and 298 nm³. A higher value of β' must be used to attain agreement with the data in the classical rod limit. A lower value of β' is required at $L/A > 2$, corresponding to $\langle M\rangle_w > 10^4$ g/mol. For a more flexible polymer in a good solvent such as polystyrene in toluene, this observation was explained in terms of the interpenetration function Ψ, given by

$$\Psi = A_2\langle M\rangle_w^2/4\pi^{3/2}N_A\langle s^2\rangle^{3/2} \qquad (25)$$

In the rod limit, $\langle s^2\rangle \sim \langle M\rangle^2$ such that $\Psi \sim M^{-1}$ with A_2 attaining a constant value. In other words, the small-angle neutron scattering results of Huber and Stockmayer permitted them to attribute the increase in Ψ to the effect of chain stiffness as $\langle M\rangle_w$ decreases.[39]

The present results for a semiflexible polymer also reflect the nature of this conclusion. However, we are unable to mimic exactly the $\langle M\rangle_w$ dependence of A_2 for X-500 in DMSO using the wormlike chain treatment above. This is depicted by the dashed line in Figure 9 having a slope of minus one. It is interesting that the major discrepancy lies between chains composed of 1 and 2 statistically equivalent segments. This discrepancy may have been anticipated by Yamakawa and Stockmayer who noted the shortcomings of their "double-contact approximation for very small L_r".[36]

Mention was made in the introduction of the negative temperature dependence of A_2. This observation reflects the decrease in solubility of X-500 in DMSO and hence poorer solvent conditions at higher temperatures.[3] In addition, the persistence length is very likely to be temperature dependent. A rough estimate of $d \ln q/dT$ from the $[\eta]$ data of ref 3 yields -4.4×10^{-3} Å/°C. This value is in excellent agreement with semiflexible thermotropic polymers.[40]

Values of q found in the present study are summarized in Table VII. A q of 105 ± 10 Å is determined by averaging the four results. This value for the persistence length of X-500 in DMSO is in excellent agreement with other workers who did not apply a correction for chain expansion in a good solvent.[11-13] We conclude, therefore, that the dimensions of X-500 in DMSO are unperturbed by excluded-volume effects and that the unperturbed dimensions must decrease with increasing temperature.

Table VII
Present Experimental Results for the Persistence Length of X-500 in DMSO

method	q, Å	method	q, Å
intrinsic viscosity	80	molecular anisotropy	110
radius of gyration	120	diffusion coefficient	110

Acknowledgment. We express our appreciation to the Monsanto Co. for supporting this research with a Graduate

Fellowship Award. We are also pleased to acknowledge the support of the National Science Foundation under Grant DMR-841 9803.

Registry No. (4-Aminobenzoic acid hydrazide)(terephthalic acid) (copolymer), 29258-54-6.

References and Notes

(1) Black, W. B.; Preston, J. *High Modulus Wholly Aromatic Fibers*; Dekker: New York, 1973.
(2) Conio, G.; Bruzzone, R.; Ciferri, A.; Bianchi, E.; Tealdi, A. *Polym. J.* **1987**, *19*, 757.
(3) Bianchi, E.; Ciferri, A.; Preston, J.; Krigbaum, W. R. *J. Polym. Sci., Polym. Phys. Ed.* **1981**, *19*, 863.
(4) Morgan, P. W. *J. Polym. Sci., Polym. Symp.* **1978**, *65*, 1.
(5) Burke, J. *J. Macromol. Sci. Chem.* **1973**, *A7*, 187.
(6) Tsvetkov, V. N.; Andreeva, L. *Adv. Polym. Sci.* **1982**, *39*, 95.
(7) Tsvetkov, V. N.; Kudriavtsev, G. J.; Miknailova, N. A.; Volokmna, A. V.; Kalmykova, V. D. *Eur. Polym. J.* **1978**, *14*, 475.
(8) Tsvetkov, V. N.; Kolomiets, I. P. Lenzov, A. V. *Eur. Polym. J.* **1982**, *18*, 373.
(9) Bianchi, E.; Ciferri, A.; Tealdi, A.; Krigbaum, W. R. *J. Polym. Sci., Polym. Phys. Ed.* **1979**, *17*, 2091.
(10) Krigbaum, W. R.; Sasaki, S. *J. Polym. Sci., Polym. Phys. Ed.* **1981**, *19*, 1339.
(11) Tsvetkov, V. N.; Tsepelevich, S. O. *Eur. Polym. J.* **1983**, *19*, 267.
(12) Pogodina, N. V.; Starchenko, L. V.; Khrustalev, A. Z.; Tsvetkov, V. N. *Polym. Sci. USSR (Engl. Transl.)* **1984**, *26*, 2300.
(13) Sakurai, K.; Ochi, K.; Norisuye, T.; Fujita, H. *Polym. J.* **1983**, *16*, 559.
(14) Yamakawa, H. *Modern Theory of Polymer Solutions*; Harper & Row: New York, 1971.
(15) Brelsford, G. L. Ph.D. Dissertation, Duke University, 1987.
(16) Berry, G. C. *J. Polym. Sci., Polym. Symp.* **1978**, *65*, 143.
(17) Koppel, D. E. *J. Chem. Phys.* **1972**, *57*, 4814.
(18) Chu, B. *Laser Light Scattering*; Academic Press: New York, 1974.
(19) *Dynamic Light Scattering, Applications, of Photon Correlation Spectroscopy*; Pecora, R., Ed.; Plenum: New York, 1985.
(20) Kobota, K.; Chu, B. *Biopolymers* **1983**, *22*, 1461.
(21) *Particle Size Distribution. Assessment and Characterization*; Provder, T., Ed.; ACS Symposium Series: American Chemical Society, 1987.
(22) Kratky, O.; Porod, G. *Recl. Tray. Chim. Pays-Bas* **1949**, *68*, 1106.
(23) Yamakawa, H. *Annu. Rev. Phys. Chem.* **1974**, *25*, 179.
(24) Yamakawa, H. *Annu. Rev. Phys. Chem.* **1984**, *35*, 23.
(25) Yamakawa, H.; Fujii, M. *Macromolecules* **1974**, *7*, 128.
(26) Benoit, H.; Doty, P. *J. Phys. Chem.* **1953**, *57*, 958.
(27) Flory, P. J. *Principles of Polymer Chemistry*; Cornell University Press: Ithaca, NY, 1953.
(28) Arpin, M.; Strazielle, C.; Weil, G.; Benoit, H. *Polymer* **1977**, *18*, 262.
(29) Ying, Q.; Chu, B. *Makromol. Chem., Rapid Commun.* **1984**, *5*, 785.
(30) Chu, B.; Ying, Q.; Wu, C.; Ford, J. R.; Dhadal, H. S. *Polymer* **1985**, *26*, 1408.
(31) Ying, Q.; Chu, B. *Macromolecules* **1987**, *20*, 871.
(32) Yamakawa, H.; Fujii, M. *Macromolecules* **1973**, *6*, 407.
(33) Vitovskaya, M. G.; Lavrenko, P. N.; Okatova, O. V.; Astapenko, E. P.; Nikolayev, V. Y.; Kal'mykova, V. D.; Volokhina, A. V.; Kudryavtsev, G. I.; Tsvetkov, V. N. *Vysokomol. Soedin., Ser. A* **1977**, *19*, 1966.
(34) Ying, Q.; Chu, B.; Qian, R.; Bao, J.; Zhang, J.; Xu, C. *Polymer* **1985**, *26*, 1401.
(35) Selser, J. C. *Macromolecules* **1981**, *14*, 346.
(36) Yamakawa, H.; Stockmayer, W. H. *J. Chem. Phys.* **1972**, *57*, 2843.
(37) Yamakawa, H.; Shimada, J. *J. Chem. Phys.* **1985**, *83*, 2607.
(38) Zimm, B. H. *J. Chem. Phys.* **1946**, *14*, 164.
(39) Huber, K.; Stockmayer, W. H. *Macromolecules* **1987**, *20*, 1400.
(40) Krigbaum, W. R.; Brelsford, G.; Ciferri, A., manuscript in preparation.

Light-Scattering Study of Three-Component Systems. 3. Θ Point for Poly(methyl methacrylate) in the Binary Mixture 1-Chlorobutane + 2-Butanol

Mitsuo Nakata,* Yoshifumi Nakano, and Kohichiro Kawate

Department of Polymer Science, Faculty of Science, Hokkaido University, Sapporo 060, Japan. *Received July 20, 1987; Revised Manuscript Received March 1, 1988*

ABSTRACT: Light-scattering measurements have been made on the ternary system of poly(methyl methacrylate) (PMMA) in the isorefractive mixture 1-chlorobutane (BuCl) + 2-butanol (BuOH), which is a cosolvent for PMMA. For the sample with the molecular weight $M_w = 2.44 \times 10^6$ the mean-square radius of gyration $\langle s^2 \rangle$ and the second virial coefficient A_2 were determined at 40 °C as a function of the volume fraction u_2 of BuOH in the mixture. A_2 was zero near $u_2 = 0$ and 0.8 and showed a large maximum near $u_2 = 0.3$. The behavior of $\langle s^2 \rangle$ was analogous to that of A_2. For samples in the molecular weight range $M_w \times 10^{-4} = 3.66$–244 the second virial coefficient A_2 was determined at $u_2 = 0.800$ as a function of temperature. A_2 was found to vanish at 39.2 ± 0.5 °C irrespective of the molecular weight. The mean-square radius of gyration $\langle s^2 \rangle$ for $M_w = 2.44 \times 10^6$ determined at $u_2 = 0.800$ and at 39.2 °C agreed with the unperturbed one measured in the single solvent BuCl. The universal function Ψ for the excluded-volume effect obtained in the mixed solvent showed a similar behavior to those observed in single solvents.

Introduction

Ternary systems of polymer + mixed solvent exhibit many interesting features. The thermodynamic behavior of the ternary systems at infinite dilution of polymer has two characteristic features, for which the light-scattering measurement is a useful experimental means. One feature is a phenomenon of the cosolvency in which the mixture of two nonsolvents for a polymer acquires high solvent power for the polymer, comparable with that of a good solvent. Another characteristic feature of the system polymer + mixed solvent stems from the composition difference of the mixed solvent inside and outside the polymer domain. The preferential absorption was first investigated by Debye et al. to analyze the apparent molecular weight obtained by light-scattering measurements for systems polymer + solvent + precipitant.[1]

Strazielle and Benoit presented a light-scattering theory based on a molecular model and analyzed the data on the

0024-9297/88/2221-2509$01.50/0